



OIST

OKINAWA INSTITUTE OF SCIENCE AND TECHNOLOGY GRADUATE UNIVERSITY
沖縄科学技術大学院大学

Butterfly-shaped magnetoresistance in van der Waals ferromagnet Fe₅GeTe₂





Author	Tomoharu Ohta, Masashi Tokuda, Shuichi Iwakiri, Kosuke Sakai, Benjamin Driesen, Yoshinori Okada, Kensuke Kobayashi, Yasuhiro Niimi
journal or publication title	AIP Advances
volume	11
number	2
page range	025014
year	2021-02-08
Publisher	AIP Publishing
Rights	(C) 2021 Author(s).
Author's flag	publisher
URL	http://id.nii.ac.jp/1394/00001866/

doi: info:doi/10.1063/9.0000067

Butterfly-shaped magnetoresistance in van der Waals ferromagnet Fe_5GeTe_2


Cite as: AIP Advances **11**, 025014 (2021); <https://doi.org/10.1063/9.0000067>

Submitted: 20 October 2020 . Accepted: 18 January 2021 . Published Online: 08 February 2021

Tomoharu Ohta, Masashi Tokuda,  Shuichi Iwakiri, Kosuke Sakai, Benjamin Driesen,  Yoshinori Okada,  Kensuke Kobayashi, and  Yasuhiro Niimi

COLLECTIONS

Paper published as part of the special topic on [65th Annual Conference on Magnetism and Magnetic Materials](#)

 This paper was selected as Featured



View Online



Export Citation



CrossMark

ARTICLES YOU MAY BE INTERESTED IN

[Shubnikov-de-Haas oscillation and possible modification of effective mass in \$\text{CeTe}_3\$ thin films](#)

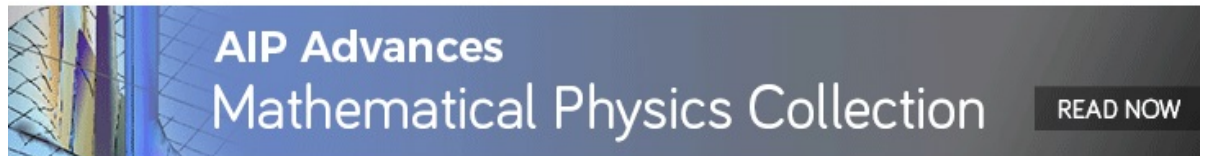
AIP Advances **11**, 015005 (2021); <https://doi.org/10.1063/9.0000074>

[Quantum oscillations with magnetic hysteresis observed in \$\text{CeTe}_3\$ thin films](#)

Applied Physics Letters **117**, 072403 (2020); <https://doi.org/10.1063/5.0007517>

[Multiple modes of a single spin torque oscillator under the non-linear region](#)

AIP Advances **10**, 075115 (2020); <https://doi.org/10.1063/5.0013105>



Butterfly-shaped magnetoresistance in van der Waals ferromagnet Fe_5GeTe_2



Cite as: AIP Advances 11, 025014 (2021); doi: 10.1063/9.0000067

Presented: 4 November 2020 • Submitted: 20 October 2020 •

Accepted: 18 January 2021 • Published Online: 8 February 2021



Tomoharu Ohta,^{1,a)} Masashi Tokuda,¹ Shuichi Iwakiri,¹ Kosuke Sakai,¹ Benjamin Driesen,² Yoshinori Okada,² Kensuke Kobayashi,^{1,3} and Yasuhiro Niimi^{1,4,b)}

AFFILIATIONS

¹Department of Physics, Graduate School of Science, Osaka University, Toyonaka, Osaka 560-0043, Japan

²Okinawa Institute of Science and Technology Graduate University, Okinawa 904-0495, Japan

³Institute for Physics of Intelligence and Department of Physics, The University of Tokyo, Bunkyo-ku, Tokyo 113-0033, Japan

⁴Center for Spintronics Research Network, Osaka University, Toyonaka, Osaka 560-8531, Japan

Note: This paper was presented at the 65th Annual Conference on Magnetism and Magnetic Materials.

Author to whom correspondence should be addressed: ohata@meso.phys.sci.osaka-u.ac.jp

^{b)}niimi@phys.sci.osaka-u.ac.jp

ABSTRACT

We have performed magnetoresistance (MR) measurements on van der Waals ferromagnetic devices using quenched- (Q-) and nonquenched- (NQ-) Fe_5GeTe_2 crystals. A clear butterfly-shaped hysteresis has been observed for thin-film (less than 6 unit-cell layer) Q- and NQ- Fe_5GeTe_2 devices, but not for thicker film ones. The switching field of the butterfly-shaped MR is consistent with the coercive field obtained from the Hall measurements. The MR ratio of the butterfly peak reaches about 10% at maximum, which is much larger than that observed with conventional magnetic materials. Such a large MR ratio would be related to magnetic fluctuations due to the complicated magnetic structure in this material.

© 2021 Author(s). All article content, except where otherwise noted, is licensed under a Creative Commons Attribution (CC BY) license (<http://creativecommons.org/licenses/by/4.0/>). <https://doi.org/10.1063/9.0000067>

I. INTRODUCTION

Recently, a group of atomic-layered materials has attracted much attentions.^{1–6} Those can be mechanically exfoliated by means of the Scotch tape method,² maintaining the high crystallinity. Therefore, they are expected to be applied to high-purity thin-film devices.^{7–12} Another attractive point is that this technique can be used for any cleavable materials with different physical properties. For example, $\text{Bi}_2\text{Sr}_2\text{CaCu}_2\text{O}_{8+\delta}$, which is known as a high-temperature cuprate superconductor, has recently been reported to show a superconducting transition for several unit-cell layers¹³ and even for a single layer.¹⁴ In addition, a ferromagnetic transition has also been demonstrated in a single (or double) layer of ferromagnetic insulator CrI_3 , ferromagnetic semiconductor $\text{Cr}_2\text{Ge}_2\text{Te}_6$, and ferromagnetic metals such as V_5Se_8 and Fe_3GeTe_2 .^{15–21} Although atomic-layered ferromagnets have been intensively studied from the viewpoint of applications such as spintronic devices, the Curie temperature T_c of these materials is still lower than room temperature.

Fe_5GeTe_2 is a newly-found atomic-layered ferromagnetic metal with T_c of 310 K in bulk.^{22–24} Therefore, it is expected to be applied to room temperature devices. However, the physical properties of Fe_5GeTe_2 are more complicated than those of similar materials such as Fe_3GeTe_2 . For example, Fe_5GeTe_2 has a similar crystal structure to Fe_3GeTe_2 , but has a larger unit-cell due to the inclusion of excess Fe atoms. In addition, Fe_3GeTe_2 shows a relatively large perpendicular magnetic anisotropy (PMA) even in bulk, and the PMA in thin film devices increases monotonically as the temperature decreases.^{19–21} On the other hand, Fe_5GeTe_2 shows almost no PMA in bulk. With decreasing the thickness of Fe_5GeTe_2 , the PMA shows up at 200 K, takes a maximum at about 120 K, and decreases as the temperature decreases.^{24,25} Furthermore, from the result of X-ray diffraction, it is known that Fe_5GeTe_2 has a structural phase transition at 550 K, and the crystal structure changes sensitively depending on how it is cooled after the sample synthesis:²³ quenched- (Q-) Fe_5GeTe_2 has a better crystallinity than nonquenched- (NQ-) one because of the metastable state. However, there are still some unclear points about the details of magnetic

structure and the relations among three different Fe sites. Therefore, further researches (especially in terms of magnetic properties of thin films) about this material are highly desirable for device applications.

In this work, we have fabricated thin film devices using both Q- and NQ- Fe_5GeTe_2 crystals and performed electrical transport measurements. A clear butterfly-shaped magnetoresistance (MR) was observed both in Q- and NQ-thin film devices. The amplitude of the MR takes a maximum at a temperature where the derivative of the longitudinal resistivity versus temperature takes a maximum. On the other hand, such an MR was not observed in Fe_5GeTe_2 devices thicker than 10 unit-cell layers (10L). These experimental results suggest that magnetic fluctuations are enhanced at a temperature where one of the Fe sites is ordered and also with decreasing the number of L of Fe_5GeTe_2 .

II. EXPERIMENTAL DETAILS

Single crystals of Fe_5GeTe_2 were synthesized in an evacuated quartz tube with iodine as a transport agent. The tube was heated up to 1050 K and kept at the temperature for a week. NQ-samples were gained by naturally cooling down them to room temperature in the quartz tube, while Q-samples were obtained by rapidly cooling down to room temperature (in detail, by dipping the tube into the water). We confirmed that both NQ- and Q-samples were single crystals by taking the X-ray diffraction pattern, and also from the energy-dispersive X-ray spectroscopy measurement. The composition ratios of Fe, Ge, and Te are 5.3, 1, and 2.4, respectively, for both NQ- and Q-samples, which hereafter we simply call Fe_5GeTe_2 . We have also confirmed that there is no iodine in the synthesized samples. From the X-ray diffraction data, the lattice constant of our samples along the *a*-axis is $a = 4.04 \text{ \AA}$ both for Q- and NQ- Fe_5GeTe_2 (see Fig. 1), while the lattice constant along the *c*-axis changes slightly depending on how we cool the samples: $c = 29.19 \text{ \AA}$ for Q- Fe_5GeTe_2 and $c = 29.04 \text{ \AA}$ for NQ- Fe_5GeTe_2 . The obtained lattice constants are consistent with those in Ref. 23.

To obtain thin film devices, we adopted the mechanical exfoliation technique using Scotch tapes in a glovebox filled with Ar gas of purity 99.9999% since exfoliated Fe_5GeTe_2 flakes are sensitive to ambient air. Some of the exfoliated Fe_5GeTe_2 flakes onto the Scotch tapes were transferred to a thermally-oxidized silicon substrate. We then coated polymethyl-methacrylate resist on the substrate and patterned electrodes with electron beam lithography. After the lithography, the substrate was put back into the glovebox for the development of the resist. Ti (5 nm) and Au (100 nm) were deposited onto the substrate in a vacuum chamber next to the glovebox, in order to take an electric contact to the flakes. We note that before the deposition of electrodes, Ar milling was performed to remove the residual resist and any possibly oxidized layers of Fe_5GeTe_2 . To prevent deterioration of the Fe_5GeTe_2 flakes, the devices were capped with PMMA shortly after the electrode deposition and the lift-off process. Thus, the devices were protected from ambient air by PMMA throughout the measurement. We determined the number of L by means of an atomic force microscopy.

III. RESULTS AND DISCUSSIONS

In Fig. 2(a), we plot the longitudinal resistivity ρ_{xx} of 5L Q- Fe_5GeTe_2 and 6L NQ- Fe_5GeTe_2 devices as a function of the

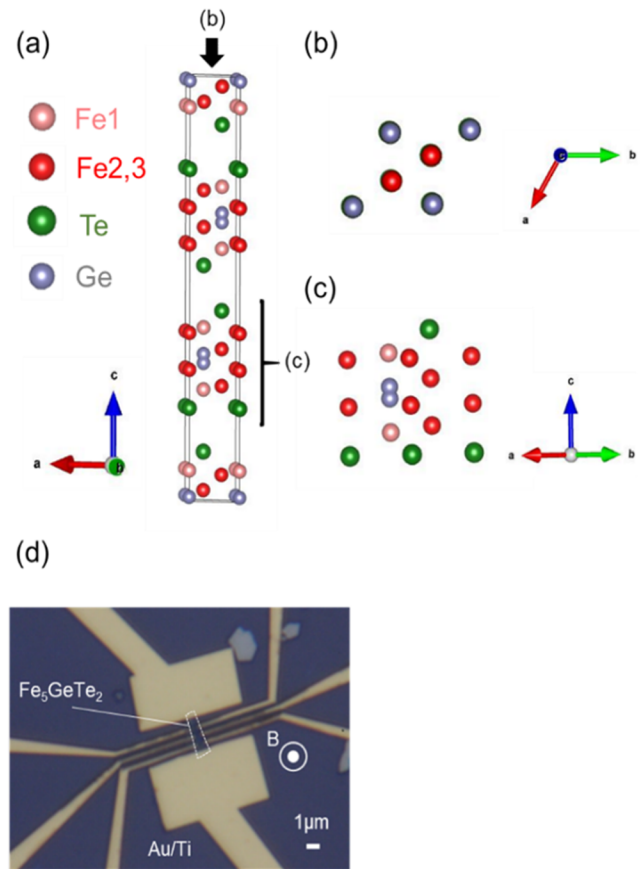


FIG. 1. (a)–(c) Schematics of crystal structure of Fe_5GeTe_2 . The black cuboid in (a) corresponds to the unit-cell of Fe_5GeTe_2 . (b) and (c) show the top and side views of a part of the unit-cell, respectively. (d) Optical microscope image of our typical device.

temperature. For both devices, a sharp drop of ρ_{xx} can be seen at around 100–120 K. This temperature region matches very well the temperature at which the Fe (1) site [see Fig. 1(a)–(c)] is ordered.^{23–25} It should be noted that the Curie temperature of 5L Q- and 6L NQ- Fe_5GeTe_2 has been determined to be about 295 K from the anomalous Hall effect measurements.²⁵ The resistivity drop of the Q-devices is sharper than that of the NQ-devices. This tendency can be seen more clearly in the derivative of ρ_{xx} versus temperature in Fig 2(b). It shows an obvious peak at 80 K (100 K) for the 5L Q- (6L NQ-) device. On the other hand, the peak becomes much broader with increasing L (more than 10 L; not shown here). These results indicate that the impact of quenching on the Fe (1) site becomes more remarkable for thinner film devices.

Next, we measured MR of Q- and NQ- Fe_5GeTe_2 devices from room temperature down to 2 K. Figure 3 shows the MR curves of 5L Q-, 6L NQ-, and 14L Q- Fe_5GeTe_2 devices obtained at 80, 100, and 110 K, respectively. Only the symmetric component is plotted in the figure to remove the Hall resistance component that could be included depending on the shape of our devices. A large butterfly-shaped hysteresis loop can be seen only near the temperature where

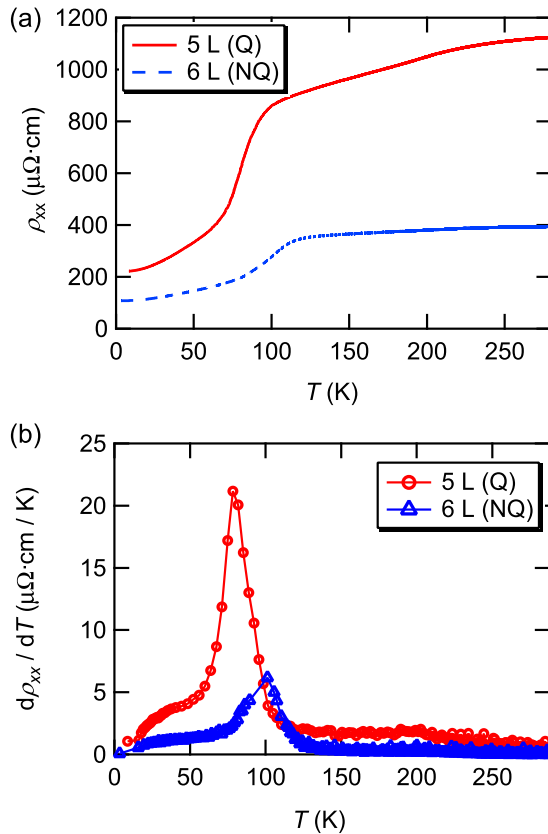


FIG. 2. (a) Temperature dependence of ρ_{xx} for 5L Q- (solid lines) and 6L NQ- (broken lines) devices. (b) Temperature dependence of the derivative of ρ_{xx} . The circle and triangle symbols indicate the results of Q- and NQ-devices, respectively.

ρ_{xx} drastically changes (see Fig. 2). The amplitude of the MR is of the order of 10%, as detailed in the next paragraph. Although it had been reported that the MR of bulk Fe_5GeTe_2 takes a maximum at around 100 K,²³ there has been no report on the observation of butterfly-shaped MR in Fe_5GeTe_2 . In addition, there are similar butterfly-shaped MRs in other ferromagnets,^{26–30} but in most cases, the amplitude of such butterfly-shape MRs is of the order of 0.1%.^{28–30} The butterfly-shaped MR in Fe_5GeTe_2 becomes much less pronounced (even vanishes) for thicker Q- and NQ-devices, as shown in Fig. 3 (see the green curve). This shows that the butterfly-shaped MR appears only in atomically-thin Fe_5GeTe_2 devices and its amplitude becomes larger for Q-devices.

Now we evaluate the peak magnitude R_{peak} and the corresponding magnetic field $|H^*|$ of the butterfly MR, which are defined in Fig. 3. In Fig. 4(a), we show R_{peak} for 5L Q- and 6L NQ-devices as a function of temperature. The overall behavior resembles Fig. 2(b). A sharp peak appears at 80 K for 5L Q-device and the maximum MR ratio reaches 10%. On the other hand, a broader peak can be seen at 100 K for 6L NQ-device and R_{peak} is about 4 times smaller than that of 5L Q-device.

In Fig. 4(b), we plot $|H^*|$ defined in Fig. 3 as a function of temperature. Although the asymmetric component has been fully

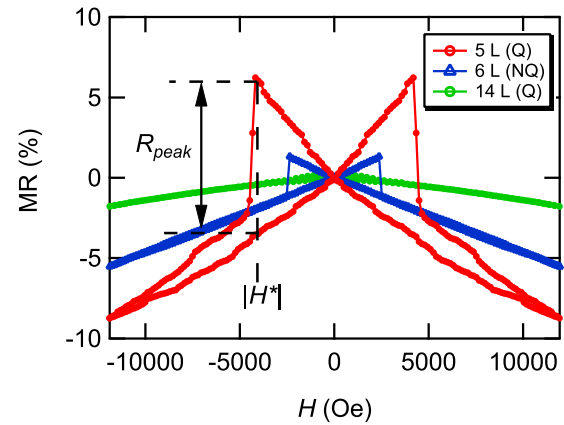


FIG. 3. MR curves of 5L Q- (red circle), 6L NQ- (blue triangle) and 14L Q- (green circle) devices taken at 80, 100 and 110 K, respectively. We define the amplitude of the butterfly-shaped MR and the corresponding magnetic field as R_{peak} and $|H^*|$ respectively.

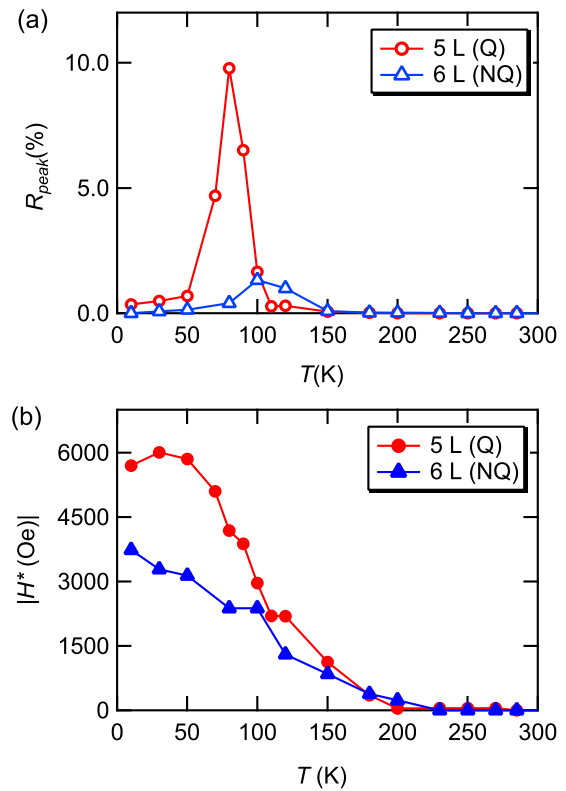


FIG. 4. (a) and (b) The amplitude of the butterfly-shaped MR (R_{peak}) and the corresponding magnetic field $|H^*|$ for 5L Q- (red circles) and 6L NQ- (blue triangles) devices as a function of temperature.

removed, the temperature dependence of H^* is very similar to the coercive field H_c obtained from the Hall measurement as detailed in in Ref. 25. The magnetization reversal in the Fe_5GeTe_2 devices occurs when we apply the external magnetic field as large as H_c .

This indicates that the observed large butterfly-shaped MR originates from the magnetization reversal of Fe_5GeTe_2 . Therefore, the reason why a clear butterfly-shaped hysteresis could not be observed in the thicker-film devices is that the PMA becomes weaker with increasing the number of L and the magnetization gradually flips. This is consistent with the Hall measurements for thicker film devices in our previous work.²⁵

Finally, let us mention the origin of the butterfly-shaped MR observed in Fe_5GeTe_2 devices. Similar butterfly-shaped MRs have already reported in FePt nanowires by Nguyen *et al.*³⁰ In that case, the MR drops when the magnetization in the nanowire flips. They attributed the MR drop to the electron-magnon scattering³¹ in the ferromagnetic nanowire. In the present case, R_{peak} takes a maximum at around 100 K and vanishes at 150 K, while the Curie temperature of the thin film Fe_5GeTe_2 is 295 K. Since the Fe (1) site is ordered at 100 K, some magnetic fluctuations should play an important role in a large MR, but at the moment it is not clear that the electron-magnon contribution discussed in Refs. 30 and 31 could play a role in the present MR. Recently, a similarly large butterfly-shaped MR (as large as 15%) has been reported³² in triangular-antiferromagnetic Ag_2CrO_2 where the magnetization switching of small remnant magnetic moments near the ordering temperature are essential. Therefore, we believe that magnetic fluctuations at the Fe (1) sites at around 100 K would be a possible origin for the butterfly-shaped MR.

IV. CONCLUSIONS

In conclusion, we have fabricated van der Waals ferromagnetic devices using both Q- and NQ- Fe_5GeTe_2 crystals, and performed MR measurements. A clear butterfly-shaped MR was observed for both Q- and NQ-thinner devices but not for thicker (more than 10L) devices. The amplitude of the MR in the Q-thinner device reaches 10%, which is much larger than those in the NQ-thinner device and in conventional ferromagnetic devices. Such a large butterfly-shaped MR indicates the enhancement of magnetic fluctuations in the Q-thinner device at a temperature where the Fe (1) site is ordered. The observed large MR hysteresis at a small switching field in atomic-layered thin film devices would be useful for future van der Waals spintronic devices.

ACKNOWLEDGMENTS

The lattice structure of Fe_5GeTe_2 was visualized using VESTA.³³ This work was supported by JSPS KAKENHI (Grant Nos. JP16H05964, JP17K18756, JP19K21850, JP26103002, JP19H00656, and JP19H05826), Mazda Foundation, Shimadzu Science Foundation, Yazaki Memorial Foundation for Science and Technology, SCAT Foundation, Murata Science Foundation, Toyota Riken Scholar, and Kato Foundation for Promotion of Science.

DATA AVAILABILITY

The data that support the findings of this study are available from the corresponding author upon reasonable request.

REFERENCES

- 1 K. S. Novoselov, D. Jiang, F. Schedin, T. J. Booth, V. V. Khotkevich, S. V. Morozov, and A. K. Geim, *Proc. Natl. Acad. Sci. USA* **102**, 10451 (2005).
- 2 J.-F. Ge, Z.-L. Liu, C. Liu, C.-L. Gao, D. Qian, Q.-K. Xue, Y. Liu, and J.-F. Jia, *Nat. Mater.* **14**, 285 (2015).
- 3 J. Shiozai, Y. Ito, T. Mitsuhashi, T. Nojima, and A. Tsukazaki, *Nat. Phys.* **12**, 42 (2016).
- 4 R. He, J. van Baren, J.-A. Yan, X. Xi, Z. Ye, I.-H. Lu, S. M. Leong, and C. H. Lui, *2D Mater.* **3**, 031008 (2016).
- 5 X. Xi, Z. Wang, W. Zhao, J.-H. Park, K. T. Law, H. Berger, L. Forró, J. Shan, and K. F. Mak, *Nat. Phys.* **12**, 139 (2016).
- 6 J. T. Ye, Y. J. Zhang, R. Akashi, M. S. Bahramy, R. Arita, and Y. Iwasa, *Science* **338**, 1193 (2012).
- 7 K. S. Novoselov and A. H. Castro Neto, *Phys. Scr.* **T146**, 014006 (2012).
- 8 A. K. Geim and I. V. Grigorieva, *Nature* **499**, 419 (2013).
- 9 K. S. Novoselov, A. Mishchenko, A. Carvalho, and A. H. Castro Neto, *Science* **353**, aac9439 (2016).
- 10 T. Song, X. Cai, M. W.-Y. Tu, X. Zhang, B. Huang, N. P. Wilson, K. L. Seyler, L. Zhu, T. Taniguchi, K. Watanabe, M. A. McGuire, D. H. Cobden, D. Xiao, W. Yao, and X. Xu, *Science* **360**, 1214 (2018).
- 11 R. Yoshimi, K. Yasuda, A. Tsukazaki, M. Kawasaki, and Y. Tokura, *Sci. Adv.* **4**, eaat9989 (2018).
- 12 M. Arai, R. Moriya, N. Yabuki, S. Masubuchi, K. Ueno, and T. Machida, *Appl. Phys. Lett.* **107**, 103107 (2015).
- 13 S. Suzuki, H. Taniguchi, T. Kawakami, M. C. Cheneau, T. Arakawa, S. Miyasaka, S. Tajima, Y. Niimi, and K. Kobayashi, *Appl. Phys. Express* **11**, 053201 (2017).
- 14 Y. Yu, L. Ma, P. Cai, R. Zhong, C. Ye, J. Shen, G. D. Gu, X. H. Chen, and Y. Zhang, *Nature* **575**, 156 (2019).
- 15 B. Huang, G. Clark, E. Navarro-Moratalla, D. R. Klein, R. Cheng, K. L. Seyler, D. Zhong, E. Schmidgall, M. A. McGuire, D. H. Cobden, W. Yao, D. Xiao, P. Jarillo-Herrero, and X. Xu, *Nature* **546**, 270 (2017).
- 16 C. Gong, L. Li, Z. Li, H. Ji, A. Stern, Y. Xia, T. Cao, W. Bao, C. Wang, Y. Wang, Z. Q. Qiu, R. J. Cava, S. G. Louie, J. Xia, and X. Zhang, *Nature* **546**, 265 (2017).
- 17 M. Nakano, Y. Wang, S. Yoshida, H. Matsuoka, Y. Majima, K. Ikeda, Y. Hirata, Y. Takeda, H. Wadati, Y. Kohama, Y. Ohigashi, M. Sakano, K. Ishizaka, and Y. Iwasa, *Nano Lett.* **19**, 8806 (2019).
- 18 Z. Fei, B. Huang, P. Malinowski, W. Wang, T. Song, J. Sanchez, W. Yao, D. Xiao, X. Zhu, A. F. May, W. Wu, D. H. Cobden, J.-H. Chu, and X. Xu, *Nat. Mater.* **17**, 778 (2018).
- 19 Y. Deng, Y. Yu, Y. Song, J. Zhang, N. Z. Wang, Z. Sun, Y. Yi, Y. Z. Wu, S. Wu, J. Zhu, J. Wang, X. H. Chen, and Y. Zhang, *Nature* **563**, 94 (2018).
- 20 Q. Li, M. Yang, C. Gong, R. V. Chopdekar, A. T. N'Diaye, J. Turner, G. Chen, A. Scholl, P. Shafer, E. Arenholz, A. K. Schmid, S. Wang, K. Liu, N. Gao, A. S. Admasu, S.-W. Cheong, C. Hwang, J. Li, F. Wang, X. Zhang, and Z. Qiu, *Nano Lett.* **18**, 5974 (2018).
- 21 S. Y. Park, D. S. Kim, Y. Liu, J. Hwang, Y. Kim, W. Kim, J.-Y. Kim, C. Petrovic, C. Hwang, S.-K. Mo, H.-J. Kim, B.-C. Min, H. C. Koo, J. Chang, C. Jang, J. W. Choi, and H. Ryu, *Nano Lett.* **20**, 95 (2020).
- 22 J. Stahl, E. Shlaen, and D. Johrendt, *Z. Anorg. Allg. Chem.* **644**, 1923 (2018).
- 23 A. F. May, C. A. Bridges, and M. A. McGuire, *Phys. Rev. Mater.* **3**, 104401 (2019).
- 24 A. F. May, D. Ovchinnikov, Q. Zheng, R. Hermann, S. Calder, B. Huang, Z. Fei, Y. Liu, X. Xu, and M. A. McGuire, *ACS Nano* **13**, 4436 (2019).
- 25 T. Ohta, K. Sakai, H. Taniguchi, B. Driesen, Y. Okada, K. Kobayashi, and Y. Niimi, *Appl. Phys. Express* **13**, 043005 (2020).
- 26 I. Žutić, J. Fabian, and S. D. Sarma, *Rev. Mod. Phys.* **76**, 323 (2004).
- 27 J.-E. Wegrowe, D. Kelly, A. Franck, S. E. Gilbert, and J.-P. Ansermet, *Phys. Rev. Lett.* **82**, 3681 (1999).
- 28 P. Li, L. T. Zhang, W. B. Mi, E. Y. Jiang, and H. L. Bai, *J. Appl. Phys.* **106**, 033908 (2009).
- 29 A. P. Mihai, J. P. Attané, A. Marty, P. Warin, and Y. Samson, *Phys. Rev. B* **77**, 060401 (2008).

³⁰V. D. Nguyen, L. Vila, P. Laczkowski, A. Marty, T. Faivre, and J. P. Attané, *Phys. Rev. Lett.* **107**, 136605 (2011).

³¹B. Raquet, M. Viret, E. Sondergard, O. Cespedes, and R. Mamy, *Phys. Rev. B* **66**, 024433 (2002).

³²H. Taniguchi, M. Watanabe, M. Tokuda, S. Suzuki, E. Imada, T. Ibe, T. Arakawa, H. Yoshida, H. Ishizuka, K. Kobaashi, and Y. Niimi, *Sci. Rep.* **10**, 2525 (2020).

³³K. Momma and F. Izumi, *J. Appl. Cryst.* **44**, 1272 (2011).